

value except λ_1^1 . For λ_1^1 the model picks up only about $\frac{2}{3}$ of the deviation from free-electron scaling. Because of the difficulty associated with λ_1^1 , the pressure derivative for this cross section was re-determined carefully in a more direct manner as indicated in Sec. II with identical results (within experimental uncertainty). Comparing this calculation with the model based on a different value of V_{10i2} , there did not appear to be any way to adjust V_{10i2} to improve the fit to λ_1^1 without significantly degrading the fit to other orbits. This again points up the sensitiveness of model descriptions to pressure data.

In conclusion we find that a converged local-pseudopotential model fits the normal-volume Fermi surface at least as well as the nonlocal model described by KSM. In addition, our model adequately predicts the pressure derivatives of Fermi cross-sectional areas. We therefore feel that this is the simplest model yet presented for Mg possessing sufficient physical significance to account for detailed experimental data.

ACKNOWLEDGMENTS

We thank R. L. White for technical assistance and R. W. Stark for helpful discussions.

*Work supported by the U. S. Atomic Energy Commission.

¹J. B. Ketterson and R. W. Stark, Phys. Rev. **156**, 748 (1967).

²R. W. Stark, Phys. Rev. **162**, 589 (1967).

³J. C. Kimball, R. W. Stark, and F. M. Mueller, Phys. Rev. **162**, 600 (1967).

⁴W. A. Harrison, Phys. Rev. **118**, 1190 (1960).

⁵W. J. O'Sullivan, J. E. Schirber, and J. R. Anderson, Solid State Commun. **5**, 525 (1967).

⁶J. E. Schirber and W. J. O'Sullivan, Phys. Rev. **184**, 628 (1969).

⁷R. W. Stark and L. R. Windmiller, Cryogenics **8**, 272 (1968).

⁸I. M. Templeton, Proc. Roy. Soc. (London) **A292**, 413 (1966).

⁹M. L. Cohen and T. K. Bergstresser, Phys. Rev. **141**, 789 (1966).

¹⁰L. J. Slutsky and C. W. Garland, Phys. Rev. **107**, 972 (1957).

¹¹P. J. Lin and L. M. Falicov, Phys. Rev. **142**, 441 (1966).

¹²We used 10 of the 11 radii used by KSM. We were not considering γ_1^1 (90°) and used a second basal-plane cigar Fermi radius instead of the one parallel to the *c* axis used by KSM.

¹³P. -O. Löwdin, J. Chem. Phys. **19**, 1396 (1951).

¹⁴J. P. Van Dyke (unpublished).

¹⁵We infer that a similar zero-pressure fit could be obtained for any reasonable value of V_{10i2} .

¹⁶For 20-kbar lattice parameters we used $a=5.9181$ a.u. and $c=9.6040$ a.u. compared to $a=6.0260$ a.u. and $c=9.7811$ a.u. at zero pressure, which assumes volume-independent compressibilities.

¹⁷We did some preliminary calculations on the nonlocal model of KSM and found significant deviations from the free-electron value for the change in the Fermi energy in the nonlocal case.

¹⁸G. Gilat, J. Comput. Phys. (to be published); G. Gilat and L. J. Raubenheimer, Phys. Rev. **144**, 390 (1966).

¹⁹A. O. E. Animalu and V. Heine, Phil. Mag. **12**, 1249 (1965).

Experimental Charge Density of Copper*

R. J. Temkin,[†] V. E. Henrich, and P. M. Raccach[‡]

Lincoln Laboratory, Massachusetts Institute of Technology, Lexington, Massachusetts 02173
(Received 27 June 1972)

The first six charge-density form factors of crystalline copper have been measured by Bragg scattering of $\text{CuK}\alpha$ and $\text{MoK}\alpha$ x rays from copper-powder samples. Detailed studies of both the samples and the x-ray beam parameters have reliably established the experimental error at about 1%. The measured form factors are in best agreement with an augmented-plane-wave (APW) self-consistent-field calculation of Snow using $X\alpha$ Slater exchange for a value of α between 0.70 and 0.75. They are in poor agreement with an APW calculation using the Chodorow potential but agree well with a calculation by Wakoh using Slater exchange and a self-consistent procedure. It is concluded that form-factor measurements of high accuracy are a sensitive and useful test of band wave functions and crystalline potentials.

I. INTRODUCTION

The measurement of the intensity of elastic (Bragg) x-ray scattering from a solid directly determines the solid-state electron charge distribu-

tion. The experimental charge density, if found to sufficiently high accuracy, may be used to test the wave functions and charge density predicted by solid-state band computations. Since theoretical wave functions are very sensitive to the choice of

crystalline potential, the experimental charge density can be a useful test of band theory. A feature that complicates the comparison of experiment with theory is the fact that the majority of the elastic x-ray scattering is caused by the inner or core electrons, while it is experimental evidence about the outer or valence electrons that is of interest in solid-state theory. In the case of copper, an experimental error of 1% or less is imperative if the charge-density form factors are to provide a satisfactory test of the valence-electron wave functions.

Since the pioneering efforts of Weiss and De Marco¹ and Batterman,² much work has been directed toward the improvement of the accuracy of elastic-x-ray-scattering measurements. The earliest attempt at a high-accuracy measurement of the copper charge-density form factors is that of Batterman, Chipman, and De Marco³ using copper-powder samples. Their experiment, however, yielded form factors in very poor agreement with Hartree-Fock theoretical values at high momentum transfer and, as Weiss⁴ has pointed out, most likely contained some systematic error. More recent determinations of the copper form factors have been made by Jennings, Chipman, and De Marco⁵ using a perfect copper crystal and Hosoya and Yamagishi⁶ using copper-powder samples. However, these two most recent experiments are not in satisfactory agreement within the stated experimental errors, so that it is difficult to draw from them an unambiguous test of solid-state theory.

This paper reports measurements of the copper form factors to high accuracy that help to clarify the previous experimental disagreement and to provide a test for theoretical charge densities. Several recent advances in the techniques of elastic-x-ray scattering from metal powders have been utilized in order to reduce the experimental error to 1%.

II. EXPERIMENT

We have determined the first six form factors of copper on an absolute scale by measuring the Bragg scattering of premonochromated x rays from pressed-powder samples. Measurements were made at $\text{CuK}\alpha$ wavelength on a Picker diffractometer and at $\text{MoK}\alpha$ wavelength on a General Electric diffractometer. The final values of the form factor are a weighted average of the results at the two different wavelengths.

A. Equipment

The General Electric diffractometer with incident-beam monochromator used in the $\text{MoK}\alpha$ experiments has been described in a previous publication.⁷ The x-ray system used in the $\text{CuK}\alpha$ experiments consisted of four main components: a Picker 6238H high-stability generator, a Picker 3488K two-axis diffractometer with a Physmet Corp. incident-beam monochromator table, a Picker 6245 detector-electronics system, and a Humphrey Electronics 914 programmer. The total configuration of equipment is basically similar to the General Electric x-ray system.

The Picker diffractometer with incident-beam monochromator is shown schematically in Fig. 1. The Dunlee copper high-intensity line-focus tube was run at 16 kV and 20 mA in order to eliminate the $\frac{1}{2}\lambda$ beam component and to maintain a low-tube temperature. A curved-graphite monochromator crystal, ordinarily used in Norelco diffracted-beam monochromators and supplied by Advanced Metals Research, Inc., was mounted on an Electronics and Alloys eucentric goniometer head. The horizontal-beam divergence, which was 0.45° full width, was limited by a 0.010-in. slit between the graphite crystal and the beam focus and a 0.005-in. slit after the focus. The beam was limited ver-

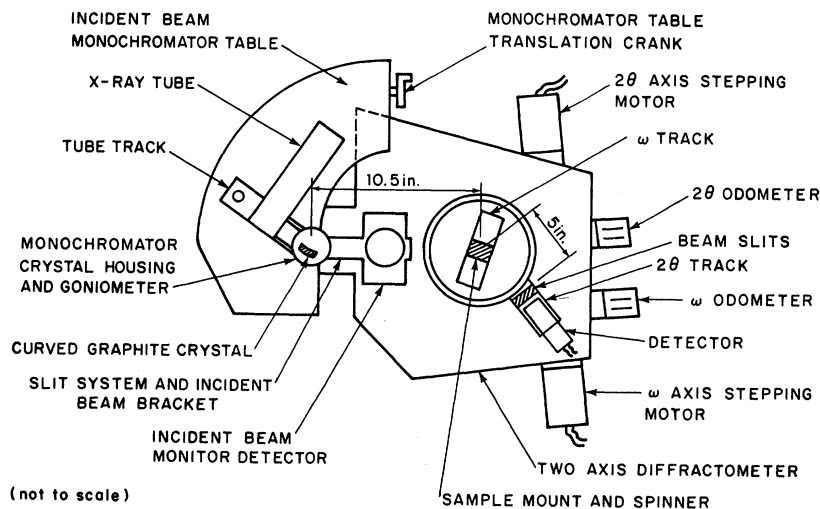


FIG. 1. X-ray diffractometer with incident-beam monochromator.

tically by a 2.0° Soller slit followed by a height slit. The scattering from a Mylar foil suspended in the monochromated x-ray beam was measured by a detector located above the foil in order to monitor the incident-beam intensity.

The incident-beam alignment was maintained within $\pm 0.02^\circ$ of 0.00° in 2θ . Copper samples were mounted on a spinner and translated along the ω track at 0.00° ω angle until the incident beam was 50% attenuated; diffracted peaks were then found to be within $\pm 0.02^\circ$ in 2θ of the expected values on both sides of the incident beam.

Both the monitor and beam detectors were integral line NaI(Tl) scintillation counters with preamplifiers; Harshaw Chemical Co. Model No. NB-18A. Encapsulated NaI(Tl) crystals, with a 0.875-in. diameter, were purchased separately from Harshaw and used only if free from clouding. Step scans of the detector through a 1×5 -mm $\text{CuK}\alpha$ beam indicated the detector response to be uniform to $\pm 0.5\%$ across the entire crystal face. Periodic checks of uniformity were carried out to determine if the crystals had been clouded by water vapor, which can very often occur within six months of manufacture. Detector pulse-height resolution was found to be 47% for $\text{CuK}\alpha$ x rays, and the dark noise was about 0.7 counts/sec.

Each counter was followed by a linear amplifier, single-channel analyzer, and scaler. The electronics deadtime for the beam counters was determined to be 2.1 ± 0.2 μsec by the foil-attenuation-vs-count-rate method described by Chipman.⁸ The data collection and diffractometer angles were controlled by a Humphrey Model No. 914 programmer with paper tape read-in and tape and card-punch output.

B. Incident-Beam Studies

The incident beams at both $\text{MoK}\alpha$ and $\text{CuK}\alpha$ wavelengths did not contain the natural ratio of $\alpha_2 : \alpha_1$ radiation. The actual ratio at each wavelength was determined by the relative peak areas of reflections from a dislocation-free germanium crystal in high order; the average wavelength was 0.7101 Å at $\text{MoK}\alpha$ and 1.5410 Å at $\text{CuK}\alpha$. The $\text{CuK}\alpha$ beam polarization was determined by the method of Jennings,⁹ in which a dislocation-free Ge crystal was scanned through the (333) reflection first in the scattering plane and then normal to the scattering plane. Correction was made for a small miscut in the Ge crystal. For the graphite monochromator a value of $k = 0.869 \pm 0.006$ was found, where k is defined as the ratio of the beam polarization in the scattering plane (π) to that normal to the plane (σ). The experimental graphite k value is between the theoretical perfect crystal (0.895) and mosaic (0.801) values. At $\text{MoK}\alpha$, a value of $k = 0.94$ was used for the LiF monochromator.

This value was somewhat arbitrarily selected, based on the argument of Jennings⁹ that secondary extinction should be larger at $\text{MoK}\alpha$ radiation. Since $\text{MoK}\alpha$ data were collected only at 2θ angles below 40° , a 5% error in k introduces less than 0.5% error in the form factor.

The monochromatic incident-beam count rate was measured after attenuation by foils with the detector fixed at 0.00° 2θ and receiving the whole beam. Two 0.003-in. brass foils were used at $\text{CuK}\alpha$ for a beam rate of about 2×10^6 sec^{-1} and five 0.005-in. Zr foils were used at $\text{MoK}\alpha$ for a beam of about 5×10^6 sec^{-1} . Of great concern at both wavelengths was the possibility of systematic errors in the I_0 count-rate determination arising from the presence of wavelengths other than the $K\alpha_1$ and $K\alpha_2$ characteristic components.

In the $\text{MoK}\alpha$ x-ray system, great care was required to prevent continuum x rays from being a source of large incident-count-rate errors. To investigate the distribution of wavelengths other than $\text{MoK}\alpha$ in the premonochromated incident beam, several tests were made. The pulse-height distribution of the $\text{MoK}\alpha$ beam was recorded for three cases: detector at $2\theta = 60.40^\circ$ for a NaCl(800) reflection of $\text{MoK}\alpha_1$; detector at 0.00° 2θ , beam attenuated by Zr foils; and detector at 0.00° 2θ , beam attenuated by brass foils. The count rate was set at 3000/sec in each case. The pulse-height distribution was measured by the usual technique of sweeping a very narrow discriminator window through the spectrum of amplified pulses from the scintillation detector. The pulse-height distributions of the first two cases were identical, but in the last case additional counts, amounting to about 1–2% of the $K\alpha$ peak, were found at higher discriminator settings (i.e., higher energies). These counts were attributed to high-energy continuum radiation, which is only weakly attenuated by brass foils. The continuum x rays were effectively reduced by using narrow discriminator windows.

After narrowing the discriminator windows the purity of the $\text{MoK}\alpha$ monochromatic incident beam was also checked by comparison of foil attenuation in the one- and two-crystal positions. These configurations are shown schematically in Fig. 2. In the one-crystal position, a uniform brass foil was placed in the premonochromated incident beam together with Zr foils, and the detector was set at 0.00° 2θ . In the two-crystal position, the brass foil remained fixed, the Zr foils were removed, and a copper-powder sample was set up for a (111) reflection into the detector with a wide receiving slit. A powder sample was selected in order to preserve the original $\alpha_1 : \alpha_2$ ratio. The attenuation of the same brass foil was measured in both the one- and two-crystal positions and was found to agree within experimental accuracy, 0.2%. This

agreement is interpreted as proof that the incident beam is sufficiently monochromatic for an accurate measurement of the beam count rate in the one-crystal position by the foil attenuation method. Establishing the wavelength purity of the incident beam is necessary if large systematic errors in measuring the incident-beam count rate are to be avoided.

C. Sample Studies

Pellets with a 1-in diameter and 0.10–0.25-in. thickness were pressed from 1- μ particle-size powder supplied by Ventron Corp. The particle size was confirmed by measurement with a Leitz metallograph. The stated powder purity was 99.9% for metallic impurities and 99% for total impurities. A diffractometer scan of the powder, which was reddish black in color, indicated that about 4% of the powder was CuO, with oxygen therefore constituting about a 1% impurity by weight. The oxygen was removed by reducing the powder in an 85%–argon–15%–hydrogen atmosphere at 300 °C for about 10 min. The criterion for termination of the reduction was a change in the powder color to bright pink. Mass spectrograph studies indicated the reduced powder purity to be better than 99.9%.

Since the pellets were exposed to the air during the x-ray measurements, it was important to determine the rate at which the sample reoxidized. Freshly reduced samples showed no evidence of CuO and Cu₂O peaks; but after two to six weeks, measurable CuO peaks indicating 0.2% oxidation appeared. Comparison of Cu(111) peaks measured within 1 h of reduction with measurements two or three months later indicated no change, and the effects of oxidation were considered negligible.

To investigate the possibility of grain growth during the reduction process, oxidation-free pellets were prepared by three methods. In the first method, powder in a tray was reduced in the Ar-H atmosphere, cooled, shaken in a jar to break up any weak sintering, and then pressed into pellets. In the second method, the pellets were pressed from the original partially oxidized powder and then reduced in the oven for a minimum time, about 10 min. A third technique was to leave reduced pellets in the oven for extended time spans, up to 40 h.

It was found that pellets prepared by all three methods gave the same integrated Bragg intensity within experimental error 1%. Pellets prepared by the first method, however, were found to have slightly more scattering in the tail of the Bragg peaks than those formed at the same pressure by the other methods.

The powder pellets were formed by uniaxial pressure in a fixed 1-in.-diam die with one fixed piston and one movable piston. Most pellets were

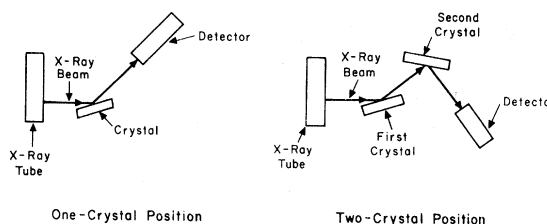


FIG. 2. Schematic representation of one-crystal and two-crystal positions used to test the spectral purity of the incident beam.

formed in the pressure range 20–150 kpsi. The pellet density α relative to that of bulk copper was, for example, 0.60 at 20 kpsi, 0.80 at 60 kpsi, and 0.94 at 150 kpsi. In order to check for porosity, the Cu-K-shell fluorescent intensity of each pellet relative to the value of a bulk standard R^* was measured, as suggested by Weiss.⁴ The samples were placed on the MoK α diffractometer and the Cu-K intensity was measured at $2\theta = 40^\circ$, 90° , and 120° , the values found being consistent to $\pm 0.2\%$. The value of R^* was 99.5% for a 20-kpsi pellet and 99.7% for a 60-kpsi pellet. No correction was made for the slight reduction of R^* below 100%, but the error limits were increased to allow for possible intensity reduction from porosity.

Metallic-powder pellets which are formed at high pressure can exhibit preferred orientation effects of the microcrystallites due to plastic flow under pressure. One method for investigating preferred orientation is to measure the intensity of diffracted peak versus pressure of pellet formation.^{3,7} It was found that pellets formed in the range 20–60 kpsi exhibited no variation in Bragg intensities with pressure, while the Bragg intensities of a 150-kpsi pellet were altered by several percent. In addition, the polar axis densities of the first three reflections of one 60-kpsi sample were measured at CuK α wavelength. This method was recently developed by Jarvinen *et al.*¹⁰ The pellet was mounted on a General Electric quarter-circle orienter that was fixed on the Picker diffractometer. The pellet was spun during the measurements, and the axis density was measured to polar axis angles up to 45° away from the vertical. No variation in Bragg intensities with polar angle was observed, and a limitation of 1% was thereby placed on preferred orientation.

Another test of the samples was the observation of the Bragg-scattered intensities as a function of the angle of x-ray beam incidence θ_i and reflection θ_o . The intensity of any Bragg reflection should vary as $2(1 + \sin\theta_i / \sin\theta_o)^{-1}$. In the usual diffraction geometry, θ_i equals θ_o . Measurements at CuK α on the (111) reflection indicated the expected

variation of peak intensity with θ_i to 0.2% accuracy down to glancing angles of about 8° . Between 5° and 8° , intensities were as much as 1% low, most likely the result of porosity and surface roughness. The (θ_i, θ_0) variation also tests preferred orientation in the same way as a polar-axis density measurement.

Finally, the effects of extinction should be negligible for our powder samples because of the small particle size used, 1μ . The agreement of Bragg intensities at the two different wavelengths and at different pellet-formation pressures is also evidence against extinction.

D. Mass Absorption Coefficient

The linear mass absorption coefficient $\mu(\lambda)$ of copper was measured at both $\text{CuK}\alpha$ and $\text{MoK}\alpha$ wavelengths. The absorption R of foils of known thickness t was measured by the foil-in-foil-out technique with corrections for deadtime and dark noise. The value of μ was then determined from the relation $R = e^{-\mu t}$. Foils of approximate thickness 0.001 and 0.005 in. were measured at $\text{CuK}\alpha$, and thickness 0.001 in. at $\text{MoK}\alpha$.¹¹ The average foil thickness was obtained by weighing each foil to an accuracy of 0.1%, measuring its area (generally 0.5 to 1.0 in.²) to 0.3% accuracy with a traveling microscope, and using the known density of copper. Measurements of foil absorption were carried out in both one- and two-crystal configurations at both $\text{MoK}\alpha$ and $\text{CuK}\alpha$ in order to assure x-ray beam purity. Almost the entire area of each foil was irradiated, and absorption was measured at several azimuthal positions, in order to prevent the preferred orientation of the foils from affecting their attenuation.¹²

Table I lists the results of several recent experimental determinations of μ/ρ , where ρ is the mass density of copper. The values listed for this experiment have been changed slightly to correspond to the natural ratio of $\alpha_1 : \alpha_2$ radiation. At $\text{CuK}\alpha$ radiation, our results are in good agreement with those of Cooper,¹³ Bearden,¹⁴ and Hughes *et al.*,¹⁵ but the values of Hosoya⁵ and Baldwin *et al.*¹⁶ are over three standard deviations lower. The differences in μ/ρ cannot be explained by a variation of α_1 and α_2 components in different x-ray beams, but rather represent a fundamental experimental disagreement between the measurements of different workers. At $\text{MoK}\alpha$, our result is higher than the other values but not outside of quoted experimental error.

We have used our values of $\mu(\lambda)$ at $\text{CuK}\alpha$ and $\text{MoK}\alpha$ together with those of Cooper¹³ and Hughes¹⁵ at other wavelengths to determine an experimental curve of $\mu(\lambda)$ vs λ . Using the theory of Parratt and Hempstead¹⁷ and the experimental $\mu(\lambda)$ curve, we have determined the value of the anomalous dispersion $\Delta f'$ at $\text{CuK}\alpha$ to be -2.20 . This value is

in excellent agreement with the value -2.15 calculated by Cromer.¹⁸

E. Diffracted Beam Power

The Bragg diffracted beam power $P(s)$ is given by

$$\frac{P(s)}{P_0} = \frac{N^2 \lambda^3 |F(h, k, l)|^2 (e^2/mc^2)^2 P(\theta) m(h, k, l) \cdot L}{32\pi R \mu(\lambda)}, \quad (1)$$

where $s = (4\pi/\lambda) \sin\theta$ is the momentum transfer; P_0 is the incident-beam power; N is the number of unit cells per unit volume; λ is the wavelength; e , m are electron charge and mass, respectively; c is the speed of light; $m(h, k, l)$ is the multiplicity; L is the receiving slit height; R is the sample to receiving slit distance; $\mu(\lambda)$ is the mass absorption coefficient;

$$F(h, k, l) = \sum_j f_j \exp[2\pi i(hx/a + ky/b + lz/c)], \quad (2)$$

where the summation is over the unit cell;

$$f(s) = [f^0(s) + \Delta f' + i\Delta f''] e^{-2Bs^2}, \quad (3)$$

where $f^0(s)$ is the form factor, $\Delta f'$ and $\Delta f''$ are anomalous dispersion corrections, and $2Bs^2$ is the Debye-Waller factor. We have

$$P(\theta) = (1 + k \cos^2 2\theta)/(1 + k) \sin^2 \theta \cos \theta, \quad (4)$$

where k is defined as [polarization in scattering plane (π)]/[polarization perpendicular to scattering plane (σ)]. A small correction was made to Eq. (1) to allow for the curvature of the Debye-Scherrer ring within the rectangular receiving slit.

Equation (1) may be used to determine experimental values of $f^0(s)$ if all of the other parameters are known. The values of λ , k , and P_0 were determined experimentally, as discussed in Sec. II B, and e , m , and c are well-known physical constants. N was calculated for a lattice parameter a of 3.6147 \AA . The slit height L was measured to $\pm 0.2\%$ accuracy on a traveling microscope, while R was determined with an error of less than 0.1%. The coefficient $\mu(\lambda)$ was measured at both $\text{CuK}\alpha$ and $\text{MoK}\alpha$, as discussed above, and $\Delta f'$ at $\text{CuK}\alpha$ was obtained from the experimental $\mu(\lambda)$ curve. Values calculated by Cromer¹⁸ were used for $\Delta f''$

TABLE I. Copper mass absorption μ/ρ (cm^2/g).

Expt.	Ref.	$\text{CuK}\alpha$	$\text{MoK}\alpha$
This expt.		51.9 ± 0.4	49.9 ± 0.6
Cooper	13	51.8 ± 0.4	48.9 ± 0.8
Jennings <i>et al.</i>	5		49.1
Bearden	14	52.3 ± 0.5	
Hughes <i>et al.</i>	15	52.2 ± 0.5	
Hosoya <i>et al.</i>	6	50.6	48.3
Batterman <i>et al.</i>	3		49.2
Baldwin <i>et al.</i>	16	49.9 ± 0.7	49.0 ± 0.7

at $\text{MoK}\alpha$ and $\Delta f''$ at both wavelengths.

The Debye-Waller temperature θ_M has been determined by several techniques in recent years. A value of $(307 \pm 3)^\circ\text{K}$ was determined by x-ray experiments on powder samples,¹⁹ $(306 \pm 4)^\circ\text{K}$ by the x-ray Borrmann effect²⁰ and $(315 \pm 10)^\circ\text{K}$ ²¹ by x-ray scattering from a single crystal. A value of $(316 \pm 2)^\circ\text{K}$ ²² was deduced from thermodynamic data, while 317°K ²³ was calculated from a fit to the inelastic neutron-scattering data. At the present time, it appears that values of θ_M near 316°K are the most reliable, so that we have used $B = 0.55$, corresponding to $\theta_M = (316 \pm 1)^\circ\text{K}$, to analyze our data.

The values of $P(s)$ at each Bragg reflection were determined by a step-scan technique using long counting times at each point. The receiving slit, subtending an angle θ_R (between 0.4° and 1.6°), was stepped in angular increments of θ_R . The peak height above background was determined, and a correction was made for first-order thermal diffuse scattering (TDS), as discussed in the Appendix. At $\text{MoK}\alpha$, an extra 0.004-in. Zr foil was used between the sample and detector in measuring both P_0 and $P(s)$ in order to eliminate Cu fluorescence in the $P(s)$ measurement.

Most of the experimental errors have already been discussed. The largest errors are $\Delta P(s)/P(s) = 0.2\%$, $\Delta P_0/P_0 = 0.5\%$, $\Delta \mu(\lambda)/\mu(\lambda) = 0.8\%$ at $\text{CuK}\alpha$; $\Delta P(\theta)/P(\theta) = 0.4\%$ at $2\theta = \frac{1}{2}\pi$ for $\text{CuK}\alpha$. The combined error in the TDS and background subtraction increases from 0.1% at the (111) reflection to about 1.0% at the (400). An error of 1.0% in the intensity is allowed for the combined effects of porosity and preferred orientation. The final error in $(f^0 + \Delta f')$ is only one-half of the experimental error assigned to $|F(s)|^2$. The error in $\Delta f'$ is about 0.04. The values of $f^0(s)$ determined at $\text{CuK}\alpha$ were in good agreement with those determined at $\text{MoK}\alpha$.

The values of $f^0(s)$ are shown in the last column of Table II, together with the results of other recent experiments. The values of $f^0(s)$ shown are an average of the $\text{CuK}\alpha$ and $\text{MoK}\alpha$ values, the former being weighted twice as heavily as the latter because of greater experimental accuracy at the $\text{CuK}\alpha$ wavelength. At each wavelength, the data are an average of results for about 10 samples formed at pressures between 20 and 60 kpsi. We delay any comparison of the results of different experiments until after consideration of the free-atom form-factor calculations.

III. COMPARISON OF EXPERIMENT TO THEORY

A. Free-Atom Calculations

The form factors of the free atom can be computed to much higher accuracy than those of the

atom in the solid because in the former case only a small number of electrons (29 in copper) need be considered. Table III is a survey of recent calculations of $f^0(s)$ for the free copper atom. The computations differ in two ways. Those listed as HF or RHF use the Hartree-Fock method, while those listed as HFS or DS use the Hartree-Fock method with exchange treated in the Slater approximation. Also, those listed as RHF or DS use the Dirac equation, while those listed HF or HFS use the nonrelativistic Schrödinger equation.

From Table III it is evident that the inclusion of the Slater approximation or relativity can alter the form-factor values by several percent, a significant amount when experimental data accurate to 1% are available. Since the Doyle and Turner²⁴ calculation uses both the more exact Hartree-Fock and Dirac procedures, it is expected to be the most reliable. Recent evidence, both theoretical²⁹ and experimental,³⁰ appears to indicate that the full Slater exchange is too strong an exchange approximation.

The copper atom may be divided into 18 inner, or core, electrons and 11 outer, or valence, electrons. The latter are the ten $3d$ and one $4s$ electrons. Since the valence electrons are at larger atomic radii, their contribution to the form factor decreases more rapidly with increasing s than the core contribution because of the e^{isr} factor in the $f^0(s)$ integral. For example, the valence electrons contribute about 28% of $f^0(s)$ at the (111) reflection, but contribute less than 13% at the (400) reflection because of the higher momentum transfer. In fact, the single $4s$ electron contributes less than 0.1% of $f^0(s)$ at all reflections and is therefore not observable at the current level of form-factor experimental accuracy.

Although the present experimental form factors are measured with bound, rather than free, atoms, they still should approach the free-atom theoretical values at large momentum transfer. The agreement arises because the charge density of the atom in the solid is expected to differ from a free atom mainly in the valence-charge region, while at large s , $f^0(s)$ is only sensitive to charge in the core region. For a reasonable estimate of the solid-state effect on the valence-charge density, the experimental form factors should be within about 1% of the RHF free-atom values by $s = 6$ or 7 \AA^{-1} .

As can be seen in Table II, our results for $f^0(s)$ are in reasonably good agreement with f^0 (RHF) at the higher reflections. The data of Batterman *et al.* and Jennings *et al.* are not in good agreement. The results of Hosoya and Yamagishi are based on different values of μ than those of the present or most other experiments. If their data were scaled to the mean value of μ determined in other experiments (see Table I), they would be

TABLE II. Experimental copper form factors.^a

Copper reflection	f^0 RHF Atom theory ^b	f^0 Batterman <i>et al.</i> ^c	f^0 Hosoya and Yamagishi ^d	f^0 Jennings <i>et al.</i> ^e	f^0 This expt.
111	22.07	21.29 ± 0.34	22.02 ± 0.09	21.58 ± 0.1	21.93 ± 0.15
200	20.72	19.75 ± 0.34	20.62 ± 0.18		20.36 ± 0.15
220	16.80	16.37 ± 0.30	16.99 ± 0.13		16.70 ± 0.16
311	14.80	(14.14 ± 0.27)	14.79 ± 0.09		14.71 ± 0.17
222	14.26		14.23 ± 0.09	14.01 ± 0.1	14.18 ± 0.17
400	12.53		12.28 ± 0.45		12.33 ± 0.20
331	11.46		11.26 ± 0.05		
420	11.17		10.90 ± 0.13		
422	10.23	9.69 ± 0.38			
333/511	9.64	8.37 ± 0.40		9.41 ± 0.1	

^aAll for $B = 0.55$.^bReference 24.^cReference 3.^dReference 6.^eReference 5.

significantly higher than the free-atom form factors at large s . Because of our better agreement at high momentum transfer, free-atom form factors, as well as our use of recent advances in experimental technique, we feel our results are more reliable than earlier measurements.

In addition to the absolute scale form-factor experiments of Table II, Linkoaho *et al.*³¹ have made relative scale measurements of $f^0(s)$ of copper. Their data, when used with $B = 0.55$, are in excellent agreement with our results. Watanabe *et al.*³² have measured the first copper form factor by a high-energy electron-diffraction technique. Their value, $f(111) = 21.78 \pm 0.13$, is within one standard deviation of our result.

B. Band-Theory Calculations

A central problem of band theory is the solution, with approximations, of the Schrödinger equation in the solid. Such a solution will yield both electron energies and wave functions. Many band calculations have been carried out for copper because its filled $3d$ shell is a good test of theoretical procedures and because much experimental information is available. The recent article by Dimmock³³ contains a comprehensive review of copper band calculations. Smith³⁴ has recently measured to high accuracy the copper d -band energies by a photoemission technique.

In many band calculations, only the band energies $E(k)$ are published and these are compared to experimental band gaps, Fermi surfaces, etc. An ambiguity arises, however, because the band energies can sometimes be accurately predicted by quite different crystalline potentials and different calculational approximations. In such a case, it is valuable to investigate the band wave functions and test them experimentally. The most direct test is the experimental x-ray form factors.

In Table IV are listed the results of several calculations of the copper solid-state form factors.

The first three calculations are by Snow³⁵ using the self-consistent-field augmented-plane-wave (APW) method with $X\alpha$ exchange, which is just Slater exchange times a constant α . Arlinghaus³⁶ has calculated form factors in the APW method using the Chodorow potential.³⁷ Wakoh's³⁸ form factors were computed using the Green's-function method, Slater exchange, and a self-consistent procedure.

In Fig. 3 we compare the results of this experiment with the three Snow $X\alpha$ calculations.³⁵ Calculations are shown in which the Slater exchange was multiplied by $\alpha = 1, \frac{5}{8},$ and $\frac{2}{3}$, where we have normalized the ordinate to $\alpha = \frac{2}{3}$. The same exchange potential was used to calculate the charge density in the valence and core regions. The band structure has been determined for these three values of α , as well as for $\alpha = 0.3$ ³⁹ and $\alpha = 0.721$,⁴⁰ the last value of α being the one that minimizes the total electronic energy of the atom.⁴¹ The form factors for $\alpha = 0.721$ can probably be safely interpolated from the data in Fig. 3. The calculated band energies of the d bands of copper, particularly $(E_F - X_5)$ and $(X_5 - X_1)$, can be compared

TABLE III. Free-atom theoretical copper form factors.

Copper reflection	$\sin\theta/\lambda$	Freeman and Watson ^a HF	Hanson <i>et al.</i> ^b HFS	Cromer and Waber ^c DS	Cromer and Mann ^d HF	Doyle and Turner ^e RHF
111	0.239 58	22.14	22.36	22.37	22.08	22.07
200	0.276 65	20.76	21.03	21.04	20.72	20.72
220	0.391 24	16.78	17.14	17.16	16.76	16.80
311	0.458 77	14.82	15.12	15.22	14.75	14.80
222	0.479 17	14.24	14.57	14.65	14.20	14.26
400	0.553 30	12.47	12.74	12.86	12.42	12.53
331	0.602 94	11.39	11.71	11.76	11.41	11.46
420	0.618 60	11.13	11.42	11.49	11.12	11.17
422	0.677 65	10.17	10.40	10.48	10.14	10.23
333/511	0.718 75	9.58	9.79	9.86	9.55	9.64

^aReference 25.^cReference 28.^bReference 26.^dReference 24.^eReference 27.

to accurate values obtained in photoemission experiments.^{34,42} Agreement is good only for the $\alpha = \frac{5}{6}$ calculation. From Fig. 3, however, we see that the $\alpha = \frac{5}{6}$ calculation is in poor agreement with the experimental charge density. The theoretical form factors of Snow should probably be corrected to include relativistic effects and should be based on a core charge density calculated by the Hartree-Fock method without exchange approximation. We still estimate, however, that even with such corrections, no value of α times Slater exchange will be in good agreement with both the experimental band energies and the experimental charge density.

In Fig. 4, we compare the results of this experiment to the calculations of Arlinghaus³⁶ and Wakoh.³⁸ For clarity, the ordinate scale has been normalized to the form factors of the $\alpha = \frac{2}{3}$ Snow calculation. The band energies for the Chodorow potential have been calculated by Arlinghaus³⁶ and Burdick⁴³ using the APW method and by Segall⁴⁴ using the Green's-function method. The *d*-band energies calculated by these workers are in excellent agreement both with one another and with experiment. As can be seen from Fig. 4, however, the Chodorow potential is in very poor agreement with the experimental charge density.

Wakoh calculated the *d*-band energies by the Green's-function method using full Slater exchange and a self-consistent procedure. The calculation is in very good agreement with both the experimental band energies and charge density. It is somewhat paradoxical to us, however, that the Wakoh calculation contains the same kind of potential as the Snow APW Slater ($\alpha = 1$) calculation but results in quite different numerical values for both the band energies and charge density.

IV. CONCLUSION

We have measured the first six charge-density form factors of copper with an experimental error of about 1%. Comparison of these form factors to theory indicates that two calculations, the Snow APW $X\alpha$ Slater and the Arlinghaus APW Chodorow, do not accurately predict both the experimental

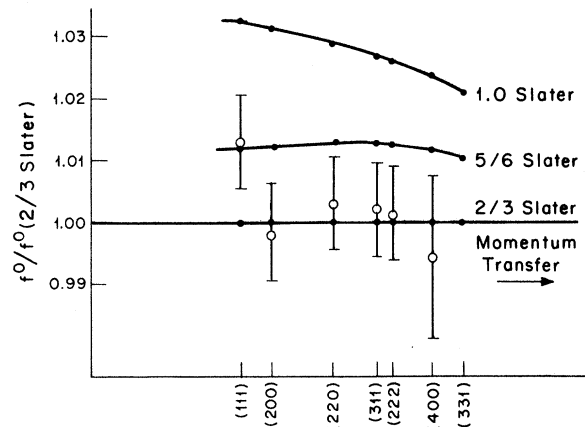


FIG. 3. Comparison of the Snow APW, SCF band theory form factors to this experiment.

band energies and charge density. The calculation of Wakoh, however, is in good agreement with both the experimental band energies and charge density. We conclude that form-factor experiments of high accuracy are a sensitive and valuable test of band calculations and band theory.

ACKNOWLEDGMENTS

One of us (R. J. T.) wishes to especially thank Professor B. Lax, his thesis supervisor, for valuable comments and advice during the course of this work. The authors would like to thank J. B. Goodenough and A. J. Strauss for many helpful discussions. We would also like to thank E. B. Owens for analyzing the samples on the mass spectrograph, J. A. Kafalas for pressing the samples, and C. H. Anderson, Jr. for assisting in many of the measurements.

APPENDIX: CORRECTION OF POWDER BRAGG PEAKS FOR TDS1

The usual correction for first-order thermal diffuse scattering (TDS1) under a powder Bragg peak is that developed by Chipman and Paskin⁴⁵ based on a theory of Warren.⁴⁶ This theory uses the Debye approximation and assumes that the velocity of all acoustic phonons in a given solid is the same. Because the TDS1 correction can amount to several percent at large momentum transfer, it was decided to investigate the adequacy of the Chipman-Paskin correction.

One weakness of the Chipman-Paskin theory is that the acoustic phonon velocities of many solids are not the same. In many materials, including copper, the longitudinal velocity v_l is about twice the transverse velocity v_t . Both the phonon-dispersion relation and phonon density of states of copper show a clear separation into longitudinal

TABLE IV. Theoretical copper form factors.

Reflection	Snow ^a	Snow ^a	Snow ^a	Arlinghaus ^b (Chodorow)	Wakoh ^c	
	$\alpha = 1$	$\alpha = \frac{5}{6}$	$\alpha = \frac{2}{3}$		Wakoh ^c	(Chodorow)
111	22.33	21.90	21.63	21.54	21.72	21.67
200	21.04	20.66	20.40	20.25	20.46	20.39
220	17.12	16.86	16.64	16.39	16.63	16.56
311	15.08	14.87	14.68	14.43	14.64	14.58
222	14.53	14.34	14.16	13.90	14.10	14.04
400	12.72	12.57	12.42	12.19	12.34	12.30
331	11.68	11.55	11.43	11.25	11.35	11.32
420	11.38	11.26	11.14	10.98	11.07	11.03
422	10.05
511/333	9.51

^aReference 35.

^bReference 36.

^cReference 38.

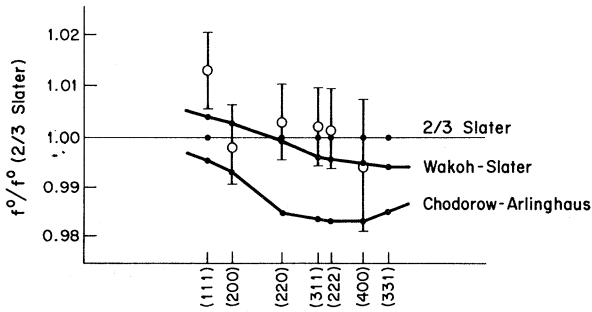


FIG. 4. Comparison of the Wakoh-Slater and Chodorow-Arlinghaus band theory form factors to this experiment.

and transverse branches.²³ A Debye theory approach, with $v_l \neq v_t$, suggested by Paskin⁴⁷ and used by him to calculate the TDS1 intensity, has been integrated here to yield the diffracted TDS1 power per angular interval and to make the TDS1 correction to the Bragg peaks.

In the Paskin formalism, θ_M and M are replaced by θ_M^D and M^D , where

$$(\theta_M^D)^2 = 3(\theta_l^{-2} + 2\theta_t^{-2})^{-1}. \quad (\text{A1})$$

θ_l and θ_t are calculated in the usual way from v_l and v_t , respectively. The total TDS1 scattered power $P_{\alpha\beta}$ (TDS1) in an angular interval from $(2\theta_0 + \alpha)$ to $(2\theta_0 + \beta)$, where $\beta > \alpha$, is obtained from the integral

$$P_{\alpha\beta}(\text{TDS1}) = \int_{\theta_0 + \alpha/2}^{\theta_0 + \beta/2} P_1(\sin\theta/\lambda) 2R d\theta, \quad (\text{A2})$$

where R is the sample to receiving slit distance and $P_1(\sin\theta/\lambda)$ is the TDS1 per unit length of diffraction circle as given in Paskin's paper.⁴⁷ The integral in Eq. (A2) cannot be done exactly, but can be done to sufficient accuracy by expanding as a function of $(\theta - \theta_0)$ and keeping only the lowest-order terms.⁴⁸ The result, valid near a Bragg peak where $(\theta - \theta_0)/\theta_0 \ll 1$, and normalized to the Bragg peak intensity $P(h, k, l)$, is

$$\frac{P_{\alpha\beta}(\text{TDS1})}{P(h, k, l)} \approx \frac{\sigma^D}{\Delta} \left[(1 + \frac{1}{3}\delta)F_{\alpha\beta} - \frac{1}{2}(\beta - \alpha) \right], \quad (\text{A3})$$

where

$$\sigma^D/\Delta = (\frac{1}{3}\pi)^{1/3} M^D(a/\lambda) \cos\theta_0, \quad (\text{A4})$$

$$\delta = 3(v_l^2/v_t^2 - 1)/(1 + 2v_l^2/v_t^2), \quad (\text{A5})$$

$$F_{\alpha\beta} = \beta[\ln(2c/\beta) + 1] - \alpha[\ln(2c/\alpha) + 1], \quad (\text{A6})$$

and

$$c = (3/\pi)^{1/3} (\lambda/2a) (1/\cos\theta_0). \quad (\text{A7})$$

If only the TDS1 above background in an angular interval between $(2\theta_0 - \beta)$ and $(2\theta_0 + \beta)$ is desired, the result is

$$\frac{P_{\beta, -\beta}(\text{TDS1 above background})}{P(hkl)} \approx \frac{\sigma^D}{\Delta} 2\beta(1 + \frac{1}{3}\delta). \quad (\text{A8})$$

Equations (A3) and (A8) are similar to the Chipman-Paskin⁴⁵ results and reduce to them for the case $v_l = v_t$. For many peaks, Eq. (A8) is adequate. When two peaks lie close together, however, Eq. (A3) should be used to correct each stepscan interval for each Bragg peak contribution.

For copper, values of $v_l = 5010$ m/sec and $v_t = 2270$ m/sec were used.⁴⁹ The Debye-Waller factor calculated from these acoustic velocities yields $\theta_M^D = 345^\circ \text{K}$, about 10% higher than the experimental value of $\theta_M = 316^\circ \text{K}$. This discrepancy is estimated to be the order of magnitude of the error involved in using the present TDS1 correction rather than one based on the actual copper phonon density of states.

Suortti⁵⁰ has developed a TDS1 correction in which a sinusoidal ω vs k relation is used instead of the linear Debye relation. He has also considered the $v_l \neq v_t$ case. We have integrated his expression for $P_1(\sin\theta/\lambda)$ to first order in $(\theta - \theta_0)$ and have found an expression for $P_{\alpha\beta}(\text{TDS1})$ slightly different from Eq. (A3). However, the result for $P_{\beta, -\beta}(\text{TDS1 above background})$ is the same as that given in Eq. (A8) for $(\theta - \theta_0) \ll \theta_0$.

*Work sponsored by the Department of the Air Force. A portion of the work was submitted by R. J. Temkin as partial fulfillment of the requirements for the degree of Doctor of Philosophy in the Physics Department, Massachusetts Institute of Technology.

†Present address: Division of Engineering and Applied Physics, Harvard University, Cambridge, Mass. 02138. Also, Physics Department, Massachusetts Institute of Technology, Cambridge, Mass. 02139.

‡Present address: Department of Physics, Belfer Graduate School, Yeshiva University, New York, N. Y. 10033.

¹R. J. Weiss and J. J. De Marco, *Rev. Mod. Phys.* **30**, 59 (1958); *Phys. Rev. Letters* **2**, 148 (1959).

²B. W. Batterman, *Phys. Rev. Letters* **2**, 47 (1959); *Phys. Rev.* **115**, 81 (1959).

³B. W. Batterman, D. R. Chipman, and J. J. De Marco, *Phys. Rev.* **122**, 68 (1961).

⁴R. J. Weiss, *X-Ray Determination of Electron Distributions* (North-Holland, Amsterdam, 1966).

⁵L. D. Jennings, D. R. Chipman, and J. J. De Marco, *Phys. Rev.* **135**, A1612 (1964).

⁶S. Hosoya and T. Yamagishi, *J. Phys. Soc. Japan* **21**, 2638 (1966).

⁷P. M. Raccach and V. E. Henrich, *Phys. Rev.* **184**, 607 (1969).

⁸D. R. Chipman, *Acta Cryst.* **A25**, 209 (1969).

⁹L. D. Jennings, *Acta Cryst.* **A24**, 472 (1968).

¹⁰M. Jarvinen, M. Merisalo, A. Pesonen, and O. Inkinen, *J. Appl. Cryst.* **3**, 313 (1970).

¹¹The foils were supplied by Ventron Corp. and were found to be better than 99.99% pure on the mass spectrom-

eter.

¹²J. J. De Marco and P. Suortti, *Phys. Rev. B* **4**, 1028 (1971).

¹³M. J. Cooper, *Acta Cryst.* **18**, 813 (1965).

¹⁴A. J. Bearden, *J. Appl. Phys.* **37**, 1681 (1966).

¹⁵G. D. Hughes, J. B. Woodhouse, and I. A. Bucklow, *Brit. J. Appl. Phys.* **1**, 695 (1968).

¹⁶T. O. Baldwin, F. W. Young, and A. Merlini, *Phys. Rev.* **163**, 591 (1967).

¹⁷L. G. Parratt and C. F. Hempstead, *Phys. Rev.* **94**, 1593 (1954).

¹⁸D. T. Cromer, *Acta Cryst.* **18**, 17 (1965).

¹⁹M. V. Linkoaho, *Phil. Mag.* **23**, 191 (1971).

²⁰C. Ghezzi, A. Merlini, and S. Pace, *Phys. Rev. B* **4**, 1822 (1971).

²¹P. A. Flinn, G. M. McManus, and J. A. Rayne, *Phys. Rev.* **123**, 809 (1961).

²²T. H. K. Barran, A. J. Leadbetter, J. A. Morrison, and L. S. Salter, *Inelastic Scattering of Neutrons in Solids and Liquids* (International Atomic Energy Agency, Vienna, 1963), Vol. I.

²³R. M. Nicklow, G. Gilat, H. G. Smith, L. J. Raubheimer, and M. K. Wilkinson, *Phys. Rev.* **164**, 922 (1967); T. O. Baldwin, *Phys. Status Solidi* **25**, 71 (1968).

²⁴P. A. Doyle and P. S. Turner, *Acta Cryst.* **A24**, 390 (1968).

²⁵A. J. Freeman and R. E. Watson, *Acta Cryst.* **14**, 231 (1961).

²⁶H. P. Hanson, F. Herman, J. D. Lea, and S. Skillman, *Acta Cryst.* **17**, 1040 (1964).

²⁷D. T. Cromer and J. T. Waber, *Acta Cryst.* **18**, 104 (1965).

²⁸D. T. Cromer and J. B. Mann, *Acta Cryst.* **A24**, 321 (1968).

²⁹N. O. Folland, *Phys. Rev. A* **3**, 1535 (1971).

³⁰P. M. Raccach and V. E. Henrich, *Intern. J. Quant. Chem.* **III**, 797 (1970).

³¹M. Linkoaho, E. Rantavuori, and U. Korhonen, *Ann. Acad. Sci. Fennicae, Ser. A* **VI**, 219 (1967).

³²D. Watanabe, R. Uyeda, and A. Fukuhara, *Acta*

Cryst. **A25**, 138 (1969).

³³J. O. Dimmock, in *Solid State Physics*, edited by H. Ehrenreich, F. Seitz, and D. Turnbull (Academic, New York, 1971), Vol. 26.

³⁴N. V. Smith, *Phys. Rev. Letters* **23**, 1452 (1969); N. V. Smith and M. M. Traum, *ibid.* **25**, 1017 (1970); N. V. Smith, *Phys. Rev. B* **3**, 1862 (1971).

³⁵J. H. Wood, in *Energy Bands in Metals and Alloys*, edited by L. H. Bennett and J. T. Waber (Gordon and Breach, New York, 1967).

³⁶F. J. Arlinghaus, *Phys. Rev.* **153**, 743 (1967), Ph. D. thesis (M.I.T., 1965) (unpublished).

³⁷M. Chodorow, *Phys. Rev.* **55**, 675 (1939); Ph. D. thesis (M.I.T., 1939) (unpublished).

³⁸S. Wakoh and J. Yamashita, *J. Phys. Soc. Japan* **30**, 422 (1971).

³⁹A. M. Boring and E. C. Snow, in *Computational Methods in Band Theory* (Plenum, New York, 1971).

⁴⁰A. M. Boring, *Phys. Rev. B* **3**, 3093 (1971).

⁴¹E. A. Kmetko, *Phys. Rev. A* **1**, 37 (1970); J. C. Slater, Present Status of the X α Statistical Exchange, Semiannual Progress Report No. 71, S.S.M.T.G. (M.I.T., 1969) (unpublished).

⁴²C. W. Berglund and W. E. Spicer, *Phys. Rev.* **136**, A1044 (1964); D. E. Eastman and J. K. Cashion, *Phys. Rev. Letters* **24**, 310 (1970).

⁴³G. A. Burdick, *Phys. Rev.* **129**, 138 (1963).

⁴⁴B. Segall, *Phys. Rev.* **125**, 109 (1961).

⁴⁵D. R. Chipman and A. Paskin, *J. Appl. Phys.* **30**, 1992 (1959); **30**, 1998 (1959).

⁴⁶B. E. Warren, *Acta Cryst.* **6**, 803 (1953); *X-Ray Diffraction* (Addison-Wesley, Reading, Mass., 1969).

⁴⁷A. Paskin, *Acta Cryst.* **11**, 165 (1958).

⁴⁸R. J. Temkin, Ph. D. thesis (M.I.T., 1971) (unpublished).

⁴⁹W. D. Mason, *Physical Acoustics and the Properties of Solids* (Van Nostrand, Princeton, N. J., 1958), p. 17.

⁵⁰P. Suortti, *Ann. Acad. Sci. Fennicae, Ser. A* **VI**, 240 (1967).

Microscopic Theory of Lattice Dynamics in Conducting Crystals*

L. J. Sham

Department of Physics, University of California, San Diego, La Jolla, California 92037

(Received 13 December 1971)

The microscopic formulation of lattice dynamics is examined in the long-wavelength limit for a general conducting crystal. Formulas for the elastic constants are derived for a complex metallic crystal.

I. INTRODUCTION

There have been an enormous number of investigations of the lattice dynamics of simple metals by the method of pseudopotentials. In this method, the crystal-structure effect is retained only in the direct ion-ion interaction; the electron screening is calculated in the homogeneous-electron-gas

approximation. This approximation is not appropriate for more or less tightly bound electrons such as the *d* electrons in the noble metals, transition metals, and their intermetallic compounds. The general formulation of the ionic and electronic contribution to lattice vibrations in crystals has been given and the long-wavelength behavior for the insulating crystals has been examined.^{1,2}